RESEARCH PAPER

Development and evaluation of miltefosine-loaded nanoemulsions on *in vitro* culture of *Toxoplasma gondii*

Gholam Reza Valizadeh [1], Mohammad Mehdi Mahboobian [2], Amir Hossein Maghsoud [1], Fatemeh Mirzaei [3], Mousa Motevali Haghi [1], Faezeh Foroughi Parvar [1], Mohammad Fallah [1]*

[1]Department of Parasitology and Mycology, Faculty of Medicine, Hamadan University of Medical Sciences, Hamadan, Iran
[2]Department of Pharmaceutics, Faculty of Pharmacy, Hamadan University of Medical Sciences, Hamadan, Iran
[3]Department of Anatomy, Faculty of Medicine, Hamadan University of Medical Sciences, Hamadan, Iran

ABSTRACT

Objective(s): *Toxoplasma gondii* is a common parasite in the world. Pharmaceutical options for toxoplasmosis treatment are limited. Several studies have been conducted on the anti-infectious properties of miltefosine (MLF). We investigated the effectiveness of nanoemulsion miltefosine (NEM) in tachyzoites of *T. gondii*, RH strain.

Materials and Methods: Various NEM formulations were designed considering pseudo-ternary phase diagrams. Physicochemical properties of the developed nanoemulsions (NEs), including pH, polydispersity index (PDI), droplet size, and refractive index (RI) were evaluated. The considered formulation was analyzed for dilution and stability tests. MTT assay was performed on Vero cells for calculation CC_{50} and on Vero cells with RH strain tachyzoite for calculation IC_{50}. Sulfadiazine (SDZ) and pyrimethamine (PYR) were positive controls. The trypan blue method was used to investigate the effect of drugs (NEM, MLF, SDZ, PYR) in reducing the number of infected Vero cells and reducing the intracellular proliferation of tachyzoites. Next, the viability of tachyzoites was measured in the tube in the direct vicinity of different drug concentrations.

Results: The final particle size of NEM was calculated to be 17.463 nm by DLS and TEM. The CC50 of NEM (75.7 µg/mL) indicated lower toxicity than the other drugs. IC_{50} obtained by trypan blue, MTT, and test tube methods showed that NEM (28.43 µg/mL) has a suitable IC_{50} against *Toxoplasma* tachyzoites.

Conclusion: The calculated selectivity index (SI) demonstrated that NEM (SI=2.66) is a more suitable drug candidate than the MLF and positive controls. The trypan blue assay indicated the excellent reduction effect of NEM on *T. gondii* intracellular proliferation rate and the number of infected cells.

Keywords: *Miltefosine, Nanoemulsion, Toxoplasma gondii, Toxoplasmosis*

How to cite this article
ValiZadeh GhR, Mahboubian MM, Maghsoud AH, Mirzaei F, Motevali Haghi M, Foroughi Parvar F, Falah M. Development and evaluation of miltefosine-loaded nanoemulsions on in vitro culture of Toxoplasma gondii. Nanomed J. 2024; 10(2):172-186. DOI: 10.22038/NMJ.2024.75808.1842

INTRODUCTION

Toxoplasma gondii is a common parasite in the world. It is expected that one-third of the global population is infected with *T. gondii* [1]. The effect of primary infection during pregnancy and its reactivation in patients with immune deficiencies is well-known; however, there are still many uncertainties regarding its diagnosis and treatment. It is estimated that 190,000 cases of congenital toxoplasmosis result in a loss of life equal to 2.1 million years (DALY) [2]. *T. gondii* consists of three strains: a) RH, b) ME49, PRU, and c) NED [3]. Infected children who are not treated may experience neurological complications and visual disorders. Reactivation of the parasite, especially in HIV-positive individuals, is a significant concern in chronic toxoplasmosis, which has been controlled in developed countries due to antiviral treatments. However, it continues to be problematic in poor and developing countries. Pharmaceutical options for treating toxoplasmosis, especially in chronic cases, are limited. Drugs that are effective against the parasite's dihydrofolate reductase (DHFR) in tachyzoite form are also

* *Corresponding author: Emails: fallah@umsha.ac.ir; mohfall@yahoo.com*
Note. This manuscript was submitted on October 24, 2023
approved on February 4, 2024

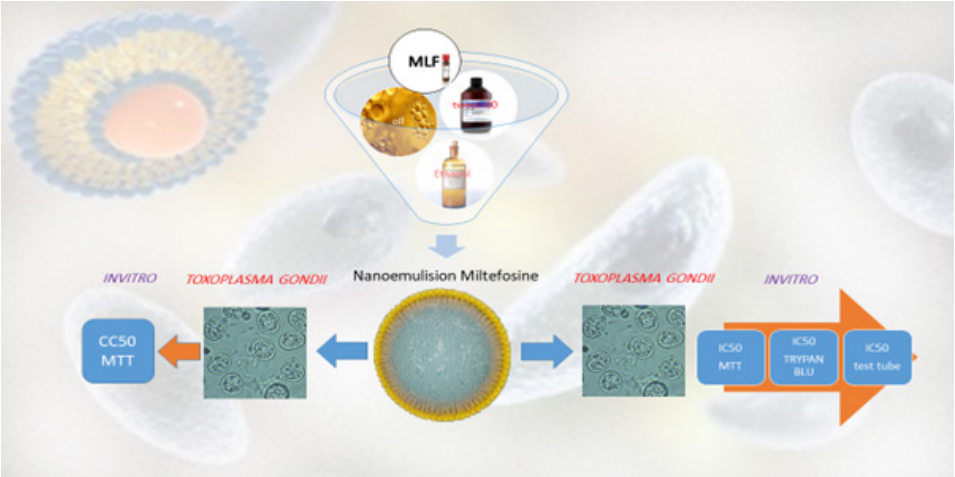

Graphical abstract. summary of the research process

effective in the acute phase, such as pyrimethamine (PYR) and trimethoprim; however, they affect human enzymes. Additionally, these drugs are ineffective when used alone and should be used in conjunction with sulfonamides that target dihydropteroate synthetase. This medication regimen can lead to myelotoxicity and pose a significant challenge for patients, such as infants or those with immune deficiencies, who require long-term treatment. Furthermore, reports of drug resistance to PYR and SDZ have been documented [4]. Other drugs, like dapsone, spiramycin, clarithromycin, azithromycin, atovaquone, and cotrimoxazole, are also employed for the clinical treatment of toxoplasmosis; however, they have no significant impact on the bradyzoite form of *T. gondii* [2]. Accordingly, identifying novel potent drug candidates effective on pregnant women and newborns with fewer side effects is essential. Ideal treatments are drugs that can disperse in the placenta and enter the fetal circulation, pass through the brain-blood barrier (BBB), spread in the central nervous system (CNS) and eyes, and be effective on cystic forms. Developing non-toxic and tolerable formulations that can suppress reactivation, shorten the therapy period, or even eradicate chronic toxoplasmosis can revolutionize the available treatment of *T. gondii*. Nanotechnology has been developed in this regard. Among established nano-based formulations, nanoemulsions (NEs) have displayed high potential as novel drug delivery vehicles [5]. NEs are associated with many advantages, including high capacity to solubilize large quantities of hydrophobic agents, low viscosity, high kinetic stability, sustained drug release pattern, and ease of sterilization [6, 7].

NEs are promising systems to increase the oral bioavailability of medications with low levels of solubility. Surfactants, oils, and an aqueous phase are mostly applied to obtain fine oil-in-water or water-in-oil NEs characterized by a droplet size < 200 nm. NEs due to their smaller droplet provide a larger surface area, leading to a higher concentration of the drug for absorption [8].

Miltefosine (MLF) is an alkyl phospholipid that acts as a metabolically stable analog of the primary phospholipid (phosphatidylcholine) found in the cell membrane of eukaryotic cells. MLF was initially synthesized in the early 1980s and considered as a treatment for cancer [9]. It was later discovered to help treat leishmaniasis, and in 2002, it was approved for this indication in India [10]. The antibacterial properties of MLF have attracted researchers' attention, particularly in cases where the bacteria are resistant to other treatments [11]. Several studies have been conducted on the antifungal [12], antiviral [13], and anti-worm [14] properties of MLF. It has also shown efficacy against metronidazole-resistant *Trichomonas vaginalis* [15], *Giardia* [16], *Entamoeba histolytica* [17], and free-living amoebae [18, 19], indicating its effectiveness against a wide range of infectious agents. MLF has a high distribution level in body tissues and a long half-life, making it beneficial in terms of pharmacokinetics. Its distribution in the brain is not well understood, but it has shown promising efficacy in treating brain parenchymal parasites, such as *Balamuthia* and *Naegleria* [20]. MLF has

also been considered an anti-HIV medication. The PI3K/Akt pathway inhibition removes HIV-infected macrophages from circulation with no effect on normal cells [13, 21]. MLF induced apoptosis in *T. gondii* [22]. MLF is listed among the essential drugs by the World Health Organization, as it is considered a safe and effective drug needed in the healthcare system [23]. A study conducted in Egypt in 2015 demonstrated the MLF effect on the tissue forms of *T. gondii*, and further research was recommended on the nano forms of MLF to increase its efficacy [24]. No effect of miltefosine nanomedicine on *T. gondii* has been reported in any published articles. Therefore, we investigated the *in vitro* effect of the new NE formulation containing MLF compared to its standard form on *T. gondii*. This is the first time such an investigation has been conducted.

MATERIALS AND METHODS

Materials

This research used MLF (molecular weight: 407.576 g·mol-1) with a chemical formula C21H46NO4P (lot#slch7768) from the Sigma Company. In the first step, the drug components underwent FTIR examination. The resulting chart was then compared to its reference chart to confirm accuracy. SDZ (lot#0000116925) and PYR (lot#BCBZ7909) were supplied by the Sigma Company. Samchun Chemical Co., Ltd, South Korea prepared Triacetin (glycerol triacetate).

Construction of pseudo-ternary phase diagrams

The considered surfactant, oil, and co-surfactant were applied to build pseudo-ternary phase diagrams by the water titration approach [25]. Tween-80 as surfactant, ethanol or Transcutol-P as co-surfactants, and triacetin as oil were mixed at different surfactant/co-surfactant mass ratios (Rsm, 2: 1, 1: 1, and 1: 2) to achieve surfactant mixture (*S*mix). Following each titration step, the clarity of the specimen was visually monitored. Mixtures characterized by optically translucent or transparent appearance were considered NE. Sigma-plot 12 software was employed to build pseudo-ternary phase diagrams.

Preparation of NE-containing MLF (NEM)

Based on the phase diagrams, systems were considered to prepare drug-loaded NEs that create a suitable region of oil-in-water NE. To prepare 1 g of drug-loaded NE systems, specific amounts of co-surfactant, surfactant, and oil were initially mixed. Then, a certain quantity of MLF (Table 1) was mixed with the resulting mixture. In the next step, after thoroughly mixing and ensuring the drug's solubility, a specified amount of water was added all at once, and the samples were stirred for 1 hr. Samples were monitored for any appearance changes during the next 72 hr.

Physicochemical characterization

The obtained NEMs were characterized as follows:

A) Droplet size and polydispersity index

The selected NEM droplet size was assessed by photon correlation spectroscopy, where the scattered light intensity was assessed by a Nanosizer (Malvern Instruments Ltd., UK) at ambient temperature.

B) Size confirmation by TEM electron microscopy

Due to the liquid nature of the samples and containing oil, first, the samples were sent to Tehran University for staining and fixation on a formvar/carbon-supported copper grid. Then the copper grid was sent to Mahamax Co.(rastak lab, sample:41826) for analysis by TEM Philips EM 208s device.

C) pH assessment

A pH meter (Boeco BT675) was applied to assess the pH of NE specimens. The assessments

Table 1. Composition of nanoemulsions containing miltefosine (MLF)

Formulation	Triacetin (Oil %)	Tween 80 (Surfactant %)	Ethanol (Co-surfactant %)	Water %	Drug %	Appearance (after 72 hr)
F1	2.5	6.67	13.3	77.38	0.15	Transparent
F2	5	6.67	13.3	74.88	0.15	Transparent
F3	7.5	6.67	13.3	72.38	0.15	Transparent
F4	2.5	10	20	67.35	0.15	Transparent
F5	5	10	20	64.85	0.15	Transparent
F6	7.5	10	20	62.35	0.15	Transparent

were performed in triplicate, and the values are reported as mean ± standard deviation (SD).

D) Refractive index (RI)

The RI of NE samples was determined using a refractometer (Fisher Scientific) device at 25°C.

Dilution test

The optimum NE samples were subjected to dilution in three different mediums, including distilled water dilutions, hydrochloric acid (pH=1.5), and phosphate buffer saline (PBS; pH=6.8). The formulation was diluted 50 and 100 times with the mentioned environments and the appearance and droplet size of the samples were evaluated.

Accelerated stability testing

Centrifugation reports and freeze-thaw and heating-cooling cycles were applied to assess the stability of the considered NEM formulations. After the tests, changes in physical instability like droplet size, opacity, drug precipitation, or phase separation were considered [26, 27].

A) Heating-cooling cycles

Samples were intermittently kept at 4°C and 40°C for six 48-hr periods.

B) Freeze-thaw cycles

Samples were intermittently kept at -21°C and 25 °C for three 48-hr periods.

C) Centrifugation

Samples then underwent centrifugation at 13000 rpm for 30 min.

In vitro study methods

Preparation of T. gondii protozoan

T. gondii (RH strain) tachyzoites were achieved from continuous intra-peritoneal injection of parasites (1×10^5) to Swiss Albino mice in the Parasitology Research Laboratory, Hamadan University of Medical Sciences. Their collection was done after washing the peritoneal cavity of animals by injecting 2 ml PBS (pH= 7.2), 100 µg/ml of streptomycin, and 100 units/ml of penicillin. Harvested fluid underwent centrifugation at 1000 g for 10 min for the removal of the peritoneal cells and debris, followed by counting tachyzoites by a hemocytometer at 2×10^4 tachyzoites per ml of sterile PBS. The isolated parasites were used for *in vitro* studies within less than 30 min (28).

Cell culture

African green monkey kidney fibroblast cells (Vero) enriched with RPMI-1640 culture (obtained from Pasteur Institute, Tehran, Iran) in addition to 10 % inactive fetal bovine serum (FBS), 100 units / mL of streptomycin and 100 units / mL of penicillin at 37 °C with 5% CO_2 in cell culture flask (surface area: 25 cm^2) were used for cell culture [29].

Investigating the toxicity of drug concentrations on Vero cells in vitro

To assess the cytotoxicity of the drugs, Vero cells (10^4 cells per 200 µL well) underwent incubation at 37 °C with 5% carbon dioxide for 24 hr. Subsequently, the cells were exposed to various levels of MLF (10, 20, 30, 40, 50, 60, 70, 80, 90, and 100 µg/mL) separately to NEM. PYR and SDZ were used as positive controls with the same concentrations. Additionally, the cells were exposed to RPMI-1640 medium containing 10% fetal bovine serum for the negative control. Ultimately, the cell viability was evaluated using the tetrazolium salt (MTT) assay and spectrophotometric analysis at 570 nm by an ELISA plate reader [28]. All experiments were performed in triplicates. The below formula was applied to convert OD to the percentage of viable cells.

$$Viability\% = \frac{\text{OD Test}}{\text{OD Control}} \times 100$$

Investigating the effect of drug concentrations on Vero cell + tachyzoite and conducting MTT assay to obtain IC_{50}

To assess the toxicity of MLF and NEM on *T. gondii* tachyzoites in Vero cells and indicate the half maximal inhibitory concentration (IC_{50}), drug concentrations of 0, 10, 20, 30, 40, 50, 60, 70, 80, 90, and 100 µg/mL were used. The tachyzoites (1×10^4) were exposed to the experimental drugs under sterile conditions and at 37 °C for 24 hr. Subsequently, the cell survival percentage and inhibition level were assessed using the MTT assay in the presence of a negative control group (*T.gondii* tachyzoites in the Vero cell and Sham) [30]. The positive control groups used PYR and SDZ with the same concentrations.

Investigating the effect of drug concentrations on in vitro intracellular T. gondii proliferation

Vero cells were seeded in plates with 24 wells with 13 mm diameter slides at 1×10^5 cells in 200 µL volume. When a confluent monolayer was obtained, Vero cells were infected by *T. gondii* tachyzoites at the ratio of 5:1. The plates underwent incubation for 3 hr with various concentrations of the experimental drugs at 37 °C [31]. Afterward, cell washing was done to eliminate extracellular

parasites. Slides were rinsed with cold, sterile saline phosphate buffer and fixed in 10% formalin for 24 hr. Staining was performed with 1% trypan blue solution for 10 sec. The number of infected cells was examined in 200 cells using light microscopy (×100) to determine the infection index. Additionally, the intracellular replication of *T. gondii* was assessed by calculating the number of parasites in 200 cells under light microscopy (×100). The inhibition percentage of *T. gondii* infection and intracellular replication in the presence of the drug was determined as below [32]:

Suppression of infection index by *T. gondii* (%) = infection index/control negative Infection index × 100 - 100

Suppression of *T. gondii* intracellular proliferation (%) = count of intracellular parasite / control negative count intracellular parasite × 100 - 100

Counting was performed twice, and the average results and the mean values were recorded in Table 6. The data were transferred to the PRISMA 8 in both xy and group formats, and the relevant analyses, including two-way ANOVA and calculation of the mean and standard error of the mean (SEM), were conducted.

Investigating the effect of drug concentrations on tachyzoites in the test tube and calculating the viability of tachyzoites in various periods

To measure the drug toxicity of *T. gondii* tachyzoites and obtain the IC_{50} value, drug doses of 10, 20, 40, 60, 80, and 100 µg/mL of MLF and separately its NE were prepared. These concentrations were exposed to 1×10^4 tachyzoites in a 1 mL suspension under sterile conditions at 37 °C for 30, 90, and 180 min. Then, 0.5 mL of the prepared parasite suspension was poured into each of the six microtubes and 0.5 mL of different drug concentrations were added to each microtube. The Negative control microtube received 0.5 mL of physiological serum, and the sham microtube received 0.5 mL of drug-free NE. PYR and SDZ with the same concentrations were used as positive control groups. The microtubes were incubated at 37 °C. Then, 30, 90, and 180 min later, the inhibitory effect of the NEM compared to the control group was calculated separately for each concentration and time point using the formula PI = (TC - TT) / TC × 100, where PI represents the inhibitory effect of the drug, TC is the number of live tachyzoites in the control group, and TT is the number of live tachyzoites at different concentrations. This experiment was done in triplicate, and the mean values were applied for calculations [29].

RESULTS AND DISCUSSION

Construction of pseudo-ternary phase diagrams

The pseudo-ternary phase diagrams of systems including triacetin and Tween 80 with two various co-surfactants (Transcutol®P & ethanol) at different regular solution models (Rsms) were constructed. As mentioned in Fig. 1, all different compositions showed an NE area that reveals appropriate compatibility between all components to form NE. Furthermore, by considering Rsm, we can conclude that regardless of co-surfactant type (Transcutol-P or ethanol), by an increase in the amount of co-surfactant, the NE region will expand; thus, the Rsm of 1:2 has the widest NE domain compared to 1:1 and 2:1. This trend has been observed in other studies [33, 34]. Finally, as the widest area was obtained at Rsm of 1:2 (Tween 80: ethanol), the composition of triacetin, Tween 80, and ethanol (1:2) was considered to develop NE formulations. Table 1 demonstrates the composition of six MLF-loaded NEs prepared by low-energy technique.

Preparation of NEs loaded with MLF

To create 1 gram of nanoemulsion systems containing the drug miltefosine, we used the optimal formula NE1 with Rsm of 1:2. First, 66.7 mg of surfactant Tween 80, 133.4 mg of cosurfactant ethanol 96, and 25 mg of triacetin oil were weighed using scales sartorius (Resolution 0.001 g). Mix them in a glass vial on a Magnetic Stirrer for 5 min. Next, 1.5 mg of miltefosine drug powder was added and mixed again for another 5 min. Finally, a 773 mg of distilled water was added to the vial and mixed on a stirrer at low speed for one hr. The formulations were stable and transparent after 72 hr at ambient temperature and evaluated.

Physicochemical characterization

Droplet size and polydispersity index

The droplet size of < 20 nm was observed for all formulations. Furthermore, their PDI was less than 0.4, which indicates the uniformity of small droplet dispersion. The small droplet size and uniformity may be attributed to the appropriate molecular arrangement of co-surfactant within the surfactant layer surrounding the oil droplets, leading to reduced interfacial tension and size reduction. The nanoscale droplet size can enhance drug delivery

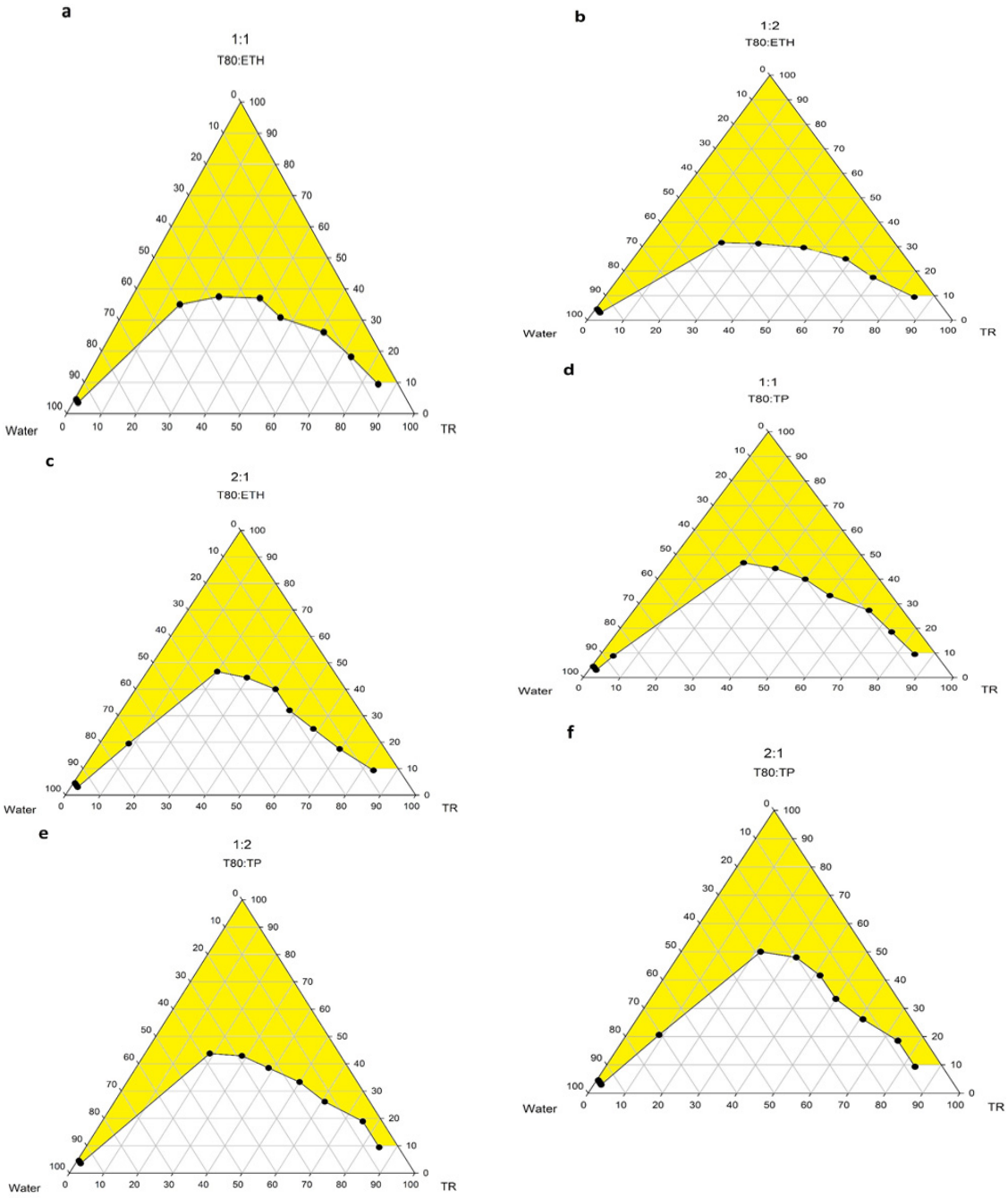

Fig. 1. Pseudo-ternary phase diagrams with various ratios of Tween 80: ethanol (a. 1:1, b. 1:2, c. 2:1) and Tween 80: Transcutol-P (d. 1:1, e. 1:2, f. 2:1). The colored region of the diagrams indicates the NE area

to target cells and improve drug permeation from the gastrointestinal epithelial cells. This allows for administering lower drug doses and fewer side effects [35].

Size verification with TEM electron microscope

TEM images displayed 20 nm diameter spherical drops (NE1). As Fig. 2 displayed, the particle sizes matched the mean sizes obtained via Nanosizer (17.463 nm), did not indicate accumulation, and had normal dispersity.

pH measurement

The pH of the formulations was determined using a pH meter at 25°C (Table 2). The pH of all formulations was between 4.53 and 4.91. Low pH

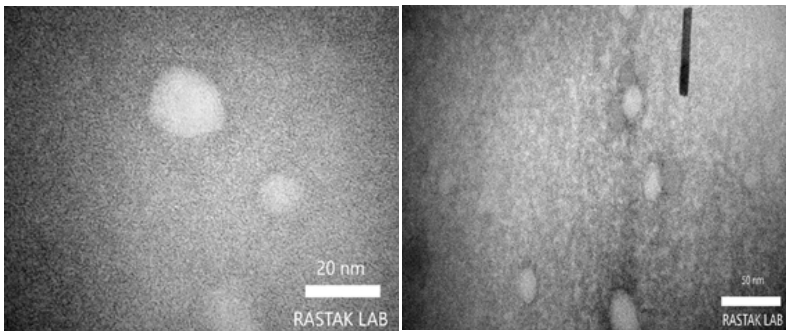

Fig. 2. Size verification with TEM Philips EM 208S electron microscope

Table 2. Physicochemical characteristics of nanoemulsions containing miltefosine (MLF) (mean ± SD; n = 3)

Formulation code	F1	F2	F3	F4	F5	F6
Droplet size (nm)	17.277 ±1.196	16.535 ±2.452	19.303 ±1.194	16.597 ±0.955	18.907 ±0.325	16.162 ±0.861
Polydispersity index (PDI)	0.260 ±0.015	0.238 ±0.046	0.289 ±0.017	0.277±0.032	0.301 ±0.002	0.270 ±0.027
pH	4.670 ±0.010	4.650 ±0.010	4.533 ±0.015	4.910 ±0.020	4.907 ±0.006	4.910 ±0.010
Refractive index (RI)	1.351 ±0.001	1.352 ±0.001	1.354 ±0.002	1.358 ±0.001	1.361 ±0.001	1.361 ±0.001

values have been reported in similar studies [36, 37]. It should be noted that these values could be adjusted around the physiologic value at 7.4.

Refractive index

The mean RI of all formulations was between 1.35 and 1.36, close to the RI of water (1.333), representing the isotropic nature of the NEs [38].

Dilution test

Table 3 presents the size and PDI values obtained from the selected formulation upon dilution ratio of 1/50 and 1/100 in various mediums, including distilled water, hydrochloric acid (pH=1.5), and PBS (pH=6.8). During the transit of NEs through the gastrointestinal (GI) tract, they face harsh conditions that can affect the structure of NEs; thus, the stability of NEs should be evaluated in similar mediums. Our findings revealed that the selected formulation (F1) could tolerate different conditions of the GI tract with no significant droplet size or PDI changes.

Table 3. Size and PDI of selected formulation (F1) after dilution test in different mediums

Dilution Formulation Code:F1	Droplet size (nm)	PDI
1/50 D.W	15.403±4.199	0.246±0.097
1/100 D.W	17.121±5.722	0.257±0.019
1/50 HCL	23.166±2.311	0.329±0.028
1/100 HCL	21.013±2.809	0.326±0.017
1/50 PBS	15.518±0.873	0.245±0.023
1/100 PBS	19.018±5.027	0.248±0.019

Accelerated physical stability assessments

Formulation F1 underwent three various stress conditions to assess physical stability. During Freeze-thaw cycles and heating–cooling cycles, and following centrifugation, no changes were observed in physical instability, like phase separation, cracking, creaming, droplet size growth (Table 4), or any turbidity.

In vitro studies

To investigate the cellular toxicity effects of the sham, SDZ, PYR, and MLF, NEM with 10 to 100 µg/ml concentrations were prepared. These samples were utilized for the following experiments.

Effect of drugs' concentrations on Vero cells to obtain CC_{50} and viability percentage

The samples were tested three times independently, and the OD readings were recorded using PRISMA 8 software. The graphs and R2 values were obtained for each time. The R2 values (NEM: 0.719, MLF: 0.878, PYR: 0.961, and SDZ: 0.997) in the analyses were close to one, indicating their

Table 4. Accelerated physical stability of the selected formulation (F1) (mean ± SD; n = 3)

Formulation	Freeze-thaw cycles		Heating-cooling cycles		Centrifugation	
	Size (nm)	PDI	Size (nm)	PDI	Size (nm)	PDI
F1	14.990± 0.388	0.306±0.013	13.247± 0.845	0.235±0.012	13.798± 1.071	0.202±0.068

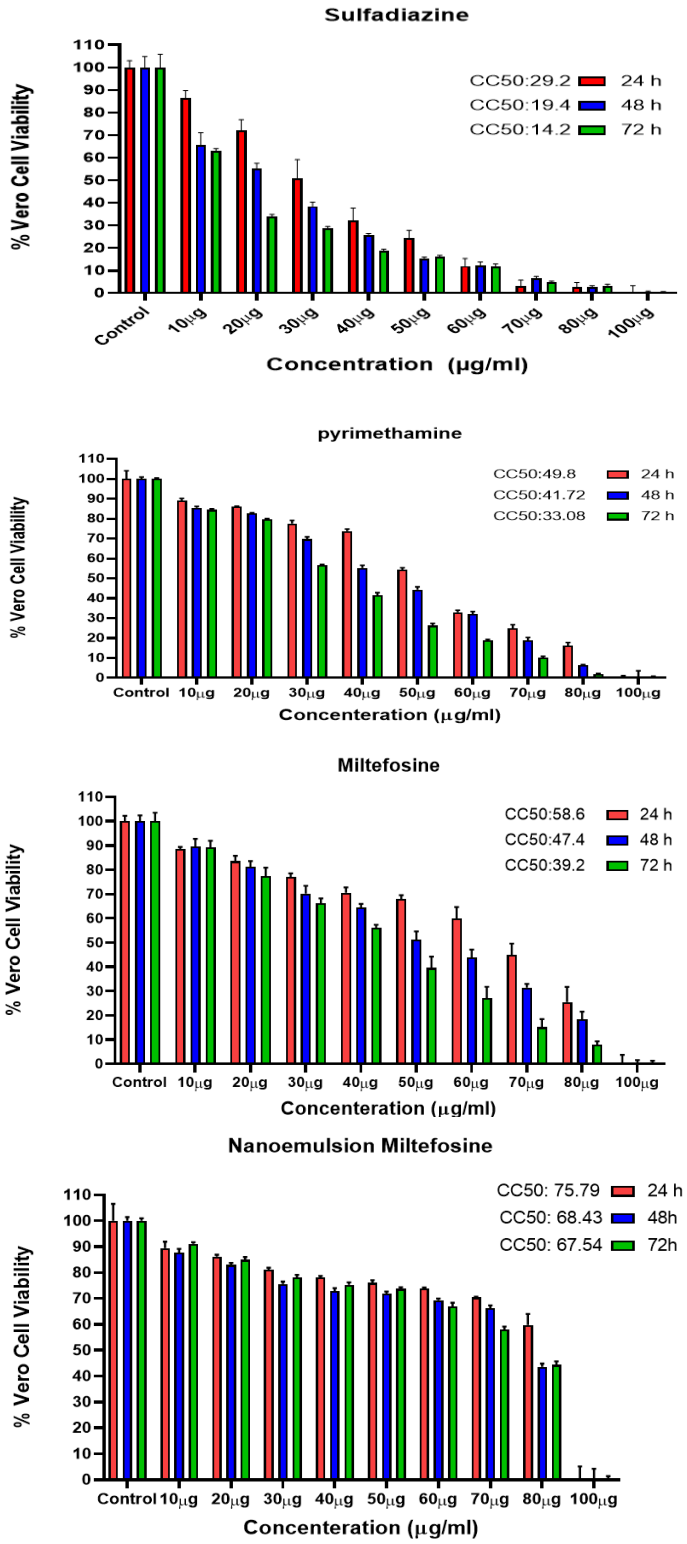

Fig. 3. Two-way ANOVA results and the significant effect of the time (24, 48, and 72 hr) and drugs' concentration on viability (P-value<0.01)

validity. Group analysis and two-way ANOVA were performed, revealing that the passage of time significantly affected cell viability in response to the drugs (P-value < 0.01) and it was decreased over time (Fig. 3). However, no significant relationship was detected between the negative control

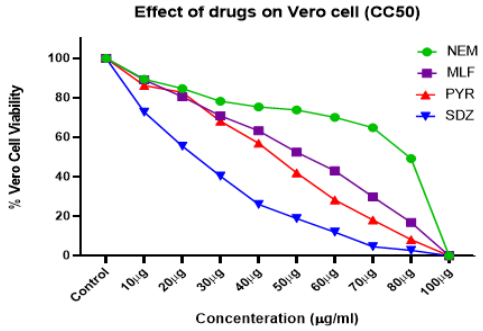

Fig. 4. Accumulative and comparative CC_{50} of the drugs: NEM: 75.7 > MLF: 58.6 > PYR: 49.8 > SDZ: 29.2

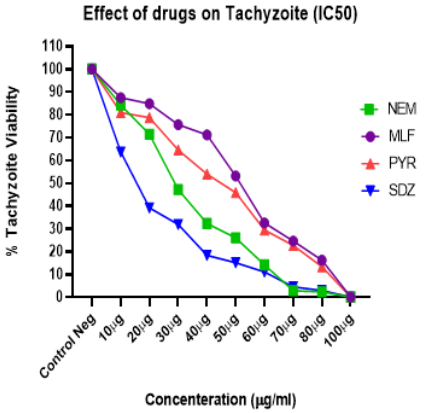

Fig. 5. Accumulative and comparative diagram of the drugs' effect on tachyzoite + Vero cell. IC_{50}: SDZ: 15.29 µg/ml < NEM: 28.43 µg/ml < PYR: 39.94 µg/ml < MLF: 48.56 µg/ml

and drug-free NE (sham) regarding the effect of elapsed time on cell viability (P-value > 0.05). In all drug groups, the increase in drug concentration caused a serial increase in cytotoxicity (P-value < 0.01). The obtained CC_{50} for each drug at 24 hr was used in the selective index (SI) formula to calculate the drug safety. The CC_{50} values of the tested drugs indicated a decrease in cellular toxicity, as illustrated in Fig. 4. It is evident that the higher the CC_{50} value, the safer the drug, particularly at higher concentrations. NEM exhibited a safer profile with a CC_{50} of 75.7 µg/mL compared to the conventional form of MLF and positive controls. In the study by Nemati et al. (2022), the cell toxicity of NeO-SLNs (Neem oil-loaded solid lipid nanoparticles) showed a direct correlation with the component concentration (P-value=0.0013). The concentration of NeO-SLNs with toxicity for at least 50% of alive *T. gondii* was > 10 mg/mL [39]. Sanfelice et al. (2021) performed an MTT assay to assess the AgNpBio cytotoxicity (Biogenic AgNPs) on HeLa cells. AgNp-Bio at different concentrations respectively decreased the viability of HeLa cells (p <0.001), than the negative control [40]. It appears that nanomedicines may cause less harm to cells by altering cytokines.

Effects of drug concentration on Vero cell +tachyzoite and MTT assay to obtain the IC_{50}

The optical absorbance of the drugs at different concentrations was recorded using PRISMA 8. The IC_{50} and R2 values were calculated. The mortality of tachyzoites was significantly enhanced by an increase in the dose of drugs (P-value <0.01). The negative control group and drug-free NE (sham) did not show a significant relationship regarding increased death and inhibition of tachyzoites (P-value>0.05). SDZ exhibited the highest efficacy in killing tachyzoites. Fig. 5 illustrates the order of potency in the lethal dose of the drug. The lower the IC_{50} value, the lower the drug dosage required to kill the parasite. However, SDZ with a CC_{50} of 29.2 µg/mL had the highest cellular toxicity among the tested drugs, and the small margin between the lethal dose IC_{50} and CC_{50} indicates its low safety profile. NEM demonstrated a higher killing potency with an IC_{50} of 28.43 µg/mL compared to PYR (39.94 µg/mL) and MLF (48.56 µg/mL) when confronted with tachyzoite + Vero cell. Because there are not many studies on the effect of MLF on *Toxoplasma*, no article was found to mention the IC_{50} of this drug against *Toxoplasma* for discussion and comparison. Future studies must pay attention to this issue.

Selectivity index calculation

The SI can be calculated by obtaining the CC_{50} from the first-stage experiments and the IC_{50} from the second-stage experiments, using the formula: SI = CC_{50} / IC_{50}. The calculated SI values for each drug are presented in Table 5. A higher SI indicates a safer drug. NEM exhibited a higher SI compared to its conventional form and positive controls,

Table 5. CC_{50} values obtained for drug effects on Vero cells and IC_{50} values obtained for drug effects on Vero cell+ tachyzoite, and calculation of selectivity index (SI) for each drug

Tested drug's name	Cytotoxicity Concentration(CC_{50}, µg/ml)	*In vitro* anti-*Toxoplasma* assay (IC_{50}, µg/ml)	SI
	(Vero + Drug)	(Vero + tachyzoite + Drug)	CC_{50}/ IC_{50}
NEM	75.70	28.43	2.66
MLF	58.60	48.56	1.20
SDZ	29.20	15.29	1.90
PYR	49.80	39.94	1.24

indicating fewer drug-related adverse effects and lower toxicity toward the treated cells.

Effect of drug concentration on in vitro intracellular T. gondii proliferation

After exposing Vero cells to tachyzoites and different drug concentrations, the cells were stained with trypan blue for 10 sec (Fig. 6). The indices related to the effect of reducing infected cells and intracellular parasitemia were calculated based on the formula provided in the methodology. Table 6 shows that the impact of the drug on reducing both indices was statistically

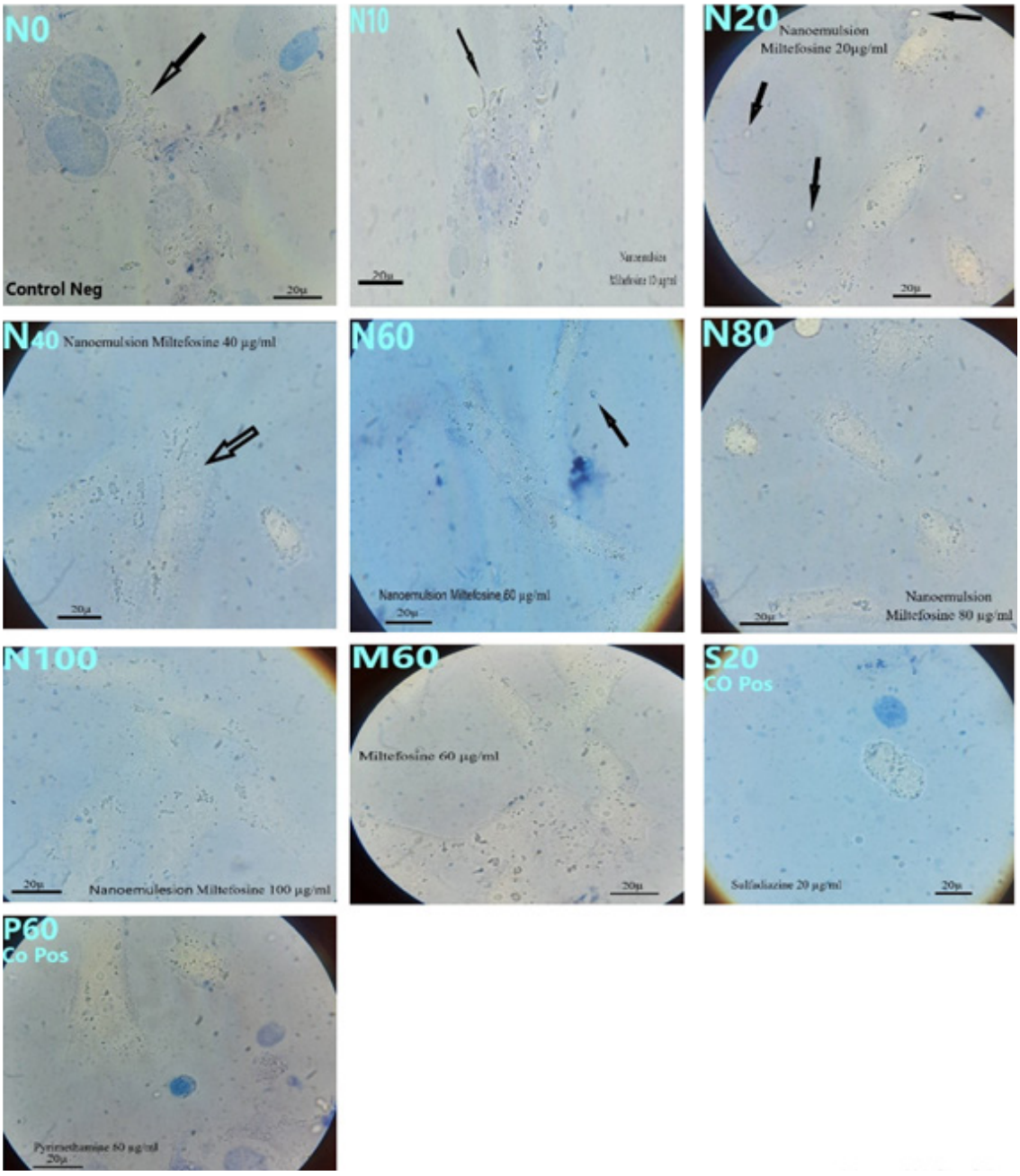

Fig. 6. Images captured using optical microscopy (HPF 100): Vero cells + tachyzoites + NEM, stained with trypan blue. As observed in the negative control, the intracellular tachyzoite regular rosette arrangement was lost in the group receiving NEM. The accumulation of tachyzoites decreased both extracellularly and intracellularly with increasing drug concentrations. The extent of reduction in intracellular and extracellular tachyzoites corresponded to the calculated IC_{50} values for all tested drugs. The images of positive control and MLF at concentrations close to IC_{50} validated the accuracy of the obtained IC_{50}. The tachyzoites are shown with arrows

Table 6. A summary of the obtained data for intracellular parasite proliferation and infection index (cell invasion) in Vero cells indicating the sum (mean ± SEM) and the inhibition (%) of the two parameters following treatment with different concentrations

Drug	Concentration µg/ml	Infection index (mean ± SEM)[a]	Inhibition of infection index by *T. gondii* (%)[c]	Parasite proliferation (mean ± SEM)[b]	Inhibition of *T. gondii,* intracellular proliferation (%)[c]
MLF	10	143.0 ±2.82	6.53	844.0±33.94	7.96
	20	112.5 ±4.94	26.47	668.50±60.10	27.09
	40	97.0 ±1.41	36.60	580.50±44.54	36.69
	60	68.5±3.53	55.22	436.50±130.81	52.39
	80	8.0±2.82	94.77	48.50±28.99	94.71
	100	1.50±0.7	99.01	8.50±4.94	99.07
NEM	10	110.0±2.82	28.10	661.50±57.27	27.86
	20	70.50±3.53	53.92	418.0±49.49	56.07
	40	42.50±3.53	72.22	248.50±31.81	72.90
	60	20.50±6.36	86.60	126.50±24.74	87.29
	80	4.50±0.7	97.05	26.50±14.84	97.98
	100	2.0±1.41	98.69	4.0±1.41	99.56
SDZ	10	105.0±5.65	31.37	665.0±65.05	26.09
	20	68.0±2.82	55.55	411.50±12.02	55.12
	40	32.0±2.82	79.00	239.50±26.16	74.97
	60	15.0±5.65	90.19	123.50±13.43	86.53
	80	5.0±2.82	96.72	22.0±5.65	97.60
	100	2.50±0.7	98.36	6.50±3.53	99.29
PYR	10	118.0±5.65	22.58	740.50±36.06	19.24
	20	72.50±6.36	52.44	423.0±33.94	53.87
	40	45.50±6.36	70.26	342.50±53.03	62.64
	60	17.0±4.24	88.88	130.50±13.43	85.76
	80	9.0±2.82	94.11	37.0±9.89	95.96
	100	2.50±2.12	98.36	8.50±2.12	99.18
Sham	0	151.0±14.56	1.300	922.0±16.68	0.0
Negative control	0	153.0±12.72	0.0	917.0±22.62	0.0

a: The number of infected cells per 200 evaluated cells; b: Intracellular proliferation of parasites: the total population of parasites per 200 evaluated cells; c: Mean population of total cell invasion or identified intracellular proliferation in cells treated with the drug The number of parasites in cells infected with *T. gondii* was reduced compared to cells infected with tachyzoites, sham, and negative control (P-value<0.01)

significant (P-value<0.05). The serial increase in drug concentrations significantly reduced both indices (P-value <0.05). Negative control and sham groups did not significantly reduce the indices. SDZ, with an IC_{50} of 15.29 µg/mL obtained from previous stage experiments, also demonstrated a greater potency (except for the 80 µg/mL concentration of NEM) in reducing the number of *T. gondii*-infected cells in this stage (Fig. 7-A). Furthermore, in other drug formulations tested, the reduction in the number of *T. gondii*-infected cells was closely correlated with the obtained IC_{50} levels. However, NEM showed a more substantial effect (except at 40 µg/mL concentration) in decreasing the number of intracellular parasites compared to other tested drugs, indicating better intracellular penetration of this drug (Fig. 7-B). The NE form of anti-*Toxoplasma* drugs has already been studied using this method with favorable results. Azami et al. (2007) assessed *in vitro* activity of atovaquone NE against *T. gondii* RH and Tehran strains, in HeLa cell culture by vital (Gimsa) staining. The atovaquone NE concentration exhibited *in vitro* anti-parasitic effects on both *T. gondii* strains (P-value <0.0001) [41]. In the study by Nemati et al. (2022), MTT assay evaluated the cell toxic effect of the component. The anti-*Toxoplasma* activity of NeO-SLNs was assessed by vital (trypan-blue) staining. Anti-intracellular *Toxoplasma* effect of NeO-SLNs was assessed on Vero cells infected by *T.gondii*. NeO-SLNs concentration-dependently could kill *T. gondii* (P-value <0.0001), and all concentrations could kill 70% of alive tachyzoites [39]. In the study by Sanfelice et al. (2021), AgNp-Bio at different levels decreased the proliferation of tachyzoites in HeLa cells than the negative control (P<0.0001). The relationship between SDZ and PYR decreased the tachyzoite proliferation in HeLa cells than the negative control [40]. There was a significant decrease in proliferation, intracellular parasitic load, and infection whereas there was an elevation in IL-6 and ROS levels. Regarding the

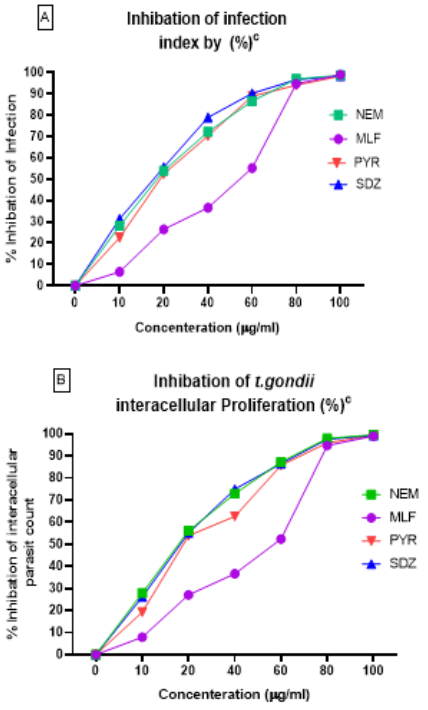

Fig. 7. Cumulative comparative effect of different concentrations of drugs on inhibition of infection (A) and intercellular proliferation (B)

action mechanisms of the parasite, AgNp-Bio can act directly on tachyzoites, induce mitochondrial membrane depolarization, increase ROS, accumulate the body's lipids, and trigger an autophagy process, leading to phosphatidylserine exposure and damage to the parasite membrane. Adeyemi et al. (2017) showed that inorganic NPs killed *T. gondii* via alterations in mitochondrial membrane potential and redox status [42]. Arruda da Silva et al. (2022) showed that biogenic AgNPs reduced *T. gondii* infection and proliferation in RAW 264.7 macrophages through tumor necrosis factor-alpha and ROS generation in the cells [43]. Quan et al. (2020) reported that AgNP-related apoptosis in ARPE-19 cells was suppressed by *T.gondii* pre-infection by inhibiting NOX4-associated ROS production [44]. Therefore, it seems that nanomedicines can speed up the destruction of tachyzoites by changes in the concentration of inflammatory mediators and cytokines.

Effect of drugs' concentrations on tachyzoites viability in the test tube

This experiment was performed three times independently, and the mean values and SEM were recorded in Table 7. The results were analyzed using PRISMA 8 according to the provided formula.

Table 7. Direct effect of the drugs on tachyzoite viability in the test tube

Groups	Concentrations µg/ml	Time						*P*-value		
		30 min		90 min		180 min			IC_{50}	SI
		Mean	SEM	Mean	SEM	Mean	SEM			
MLF	10	83.22	± 1.33	78.02	± 0.99	75.01	± 1.02	<0.05	45.86	1.27
	20	80.05	± 0.98	77.25	± 1.45	72.53	± 1.99			
	40	67.50	± 2.32	66.03	± 2.60	61.52	± 2.03			
	60	35.45	± 1.35	33.80	± 1.45	30.33	± 2.01			
	80	18.05	± 2.15	15.08	± 1.02	10.42	± 1.91			
	100	12.66	± 1.65	9.22	± 2.46	5.01	± 2.44			
NEM	10	80.30	± 1.18	76.88	± 2.14	69.04	± 1.47	<0.05	35.28	2.14
	20	69.02	± 2.33	66.25	± 1.94	58.22	± 2.22			
	40	44.40	± 1.52	40.18	± 1.52	39.00	± 1.5			
	60	22.35	± 2.13	18.20	± 2.56	10.11	±1.22			
	80	12.27	± 1.15	8.09	± 2.68	6.59	± 3.12			
	100	6.16	± 2.13	6.23	± 1.29	2.09	± 3.22			
SDZ	10	68.46	±1.38	54.02	± 1.92	50.11	± 2.88	<0.05	30.35	0.96
	20	42.45	± 2.57	34.27	± 2.03	28.90	± 3.02			
	40	20.77	± 2.38	15.90	± 2.35	10.05	± 2.05			
	60	9.63	± 1.64	8.33	± 1.33	7.64	± 2.38			
	80	5.26	± 2.55	4.33	± 1.09	3.00	± 2.08			
	100	4.20	± 1.39	2.21	± 1.44	1.50	± 2.52			
PYR	10	85.55	± 1.52	82.00	± 2.00	74.28	± 2.51	<0.05	46.77	1.06
	20	80.63	± 2.08	77.20	± 2.08	69.01	± 2.59			
	40	73.87	± 3.15	54.33	± 3.41	47.21	± 3.11			
	60	40.55	± 3.58	31.60	±3.04	24.56	± 2.99			
	80	20.06	± 1.87	14.83	± 2.71	11.36	± 2.44			
	100	10.02	± 1.52	5.03	± 2.08	3.10	± 1.98			
Sham	-	95.00	± 1.09	92.00	± 2.81	90.58	± 1.65	>0.05		
Negative control	-	96.08	± 1.33	94.33	± 1.51	92.09	± 1.82	>0.05		

The Two-Way ANOVA test with a P-value < 0.05 was performed to assess the significance of the reduction in tachyzoite viability when exposed to serial concentrations of the drug

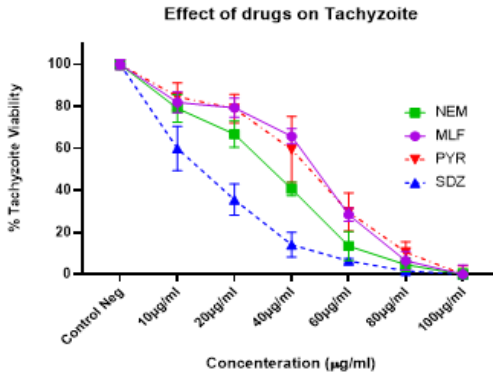

Fig. 8. The level of tachyzoite viability in direct exposure to different drug concentrations. SDZ was more effective in reducing tachyzoite viability than other drugs

Live tachyzoites remained colorless, while dead tachyzoites appeared blue. Drugs significantly affected tachyzoite viability compared to the negative control (P< 0.05). The potency of the drugs in increasing tachyzoite mortality was in the following order: PYR < MLF< NEM < SDZ (Fig. 8). The increase in drug effect was significant with increasing concentration (P<0.05). The IC_{50} values of the drugs were determined based on the concentration required for 50% tachyzoite viability. However, since the target parasite is an intracellular species, it is more accurate to calculate the IC_{50} by directly exposing the parasite to Vero cells and the drug, followed by the MTT assay. Nevertheless, the IC_{50} values obtained by this approach approximate the results of the MTT method. Furthermore, the obtained SI values indicate the relative safety of the drug. SI value for NEM was 2.14, followed by MLF (1.47), PYR (1.06), and SDZ (0.96). This highlights the lower risk associated with NEM compared to the positive controls and MLF. The sham and negative control groups had no significant effect on tachyzoite viability (P>0.05). In the study by Khamesipour et al. (2021), the effect of *D. kotschyi* essential oil (EO) against *Toxoplasma* was more significant than the negative control (P< 0.05) [29]. In addition, a significant difference was detected between the EO of *D. kotschyi* and the positive control at all concentrations and following various exposure times. In our study and this study, there is a difference regarding the effect of positive control drugs on the survival of tachyzoites. In our study, SDZ was more effective in reducing the survival of tachyzoites in direct exposure, which was consistent with the obtained IC_{50}. This issue should be considered in future studies.

CONCLUSION

The average size of less than 20 nm for NEM can effectively deliver drugs to sites, such as the brain. SI values demonstrated that the NE of MLF (SI NEM: 2.66) is a more suitable drug compared to the conventional form and positive controls. A high CC_{50} (75.7 µg/mL) of NEM when exposed to Vero cells and a suitable IC_{50} (28.43 µg/mL) against the tachyzoite + Vero cell combination indicates an effective drug with fewer side effects. The tachyzoite + Vero cells underwent trypan blue staining to evaluate the impact of different drug concentrations on the number of infected cells and intracellular replication and its results showed that NEM had a significant effect, particularly on intracellular reduction. Improved intracellular penetration of MLF as an NE formulation holds promise for combating intracellular *T. gondii*. The effectiveness of MLF in the treatment of cancer, AIDS (diseases, in which the likelihood of *T. gondii* activation is high due to immune deficiency), and toxoplasmosis, makes it a logical choice for therapeutic purposes. Because *T. gondii* cysts are predominantly formed in the brain, and the BBB poses a challenge for drug accessibility to brain tissue and the significance of treating cerebral cysts, it is recommended to assess the effect of NEM *in vivo*.

ACKNOWLEDGMENTS

This work is supported in parts financially by the Deputy for Research and Technology, Hamadan University of Medical Sciences who hereby gratefully acknowledged.

FUNDING

This research was funded by the Hamadan University of Medical Sciences [Grant No.: 140008116656].

CONFLICS OF INTEREST

The authors declare that there is no conflict of interest.

REFERENCES

1. Montoya JG, Liesenfeld O. Toxoplasmosis. Lancet. 2004;363(9425):1965-1976.
2. Montazeri M, Sharif M, Sarvi S, Mehrzadi S, Ahmadpour E, Daryani A. A Systematic Review of *In vitro* and In vivo Activities of Anti-Toxoplasma Drugs and Compounds (2006-2016). Front Microbiol. 2017;8:25.
3. Howe DK, Sibley LD. Toxoplasma gondii comprises three clonal lineages: correlation of parasite genotype with human disease. J Infect Dis. 1995;172(6):1561-1566.

4. Villena I, Aubert D, Leroux B, Dupouy D, Talmud M, Chemla C, et al. Pyrimethamine-sulfadoxine treatment of congenital toxoplasmosis: follow-up of 78 cases between 1980 and 1997. Reims Toxoplasmosis Group. Scand J Infect Dis. 1998;30(3):295-300.
5. Sahoo SK, Dilnawaz F, Krishnakumar S. Nanotechnology in ocular drug delivery. Drug Discov Today. 2008;13(3-4):144-151.
6. Gupta A, Eral HB, Hatton TA, Doyle PS. Nanoemulsions: formation, properties and applications. Soft Matter. 2016;12(11):2826-4281.
7. Ammar HO, Salama HA, Ghorab M, Mahmoud AA. Nanoemulsion as a potential ophthalmic delivery system for dorzolamide hydrochloride. AAPS PharmSciTech. 2009;10(3):808-819.
8. Gutiérrez J, González C, Maestro A, Sole I, Pey C, Nolla J. Nanoemulsions: new applications and optimization of their preparation. Curr Opin Colloid Interface Sci. 2008;13(4):245–251.
9. van Blitterswijk WJ, Verheij M. Anticancer alkylphospholipids: mechanisms of action, cellular sensitivity and resistance, and clinical prospects. Curr Pharm Des. 2008;14(21):2061-2074.
10. Dorlo TP, Balasegaram M, Beijnen JH, de Vries PJ. Miltefosine: a review of its pharmacology and therapeutic efficacy in the treatment of leishmaniasis. J Antimicrob Chemother. 2012;67(11):2576-2597.
11. Llull D, Rivas L, García E. *In vitro* bactericidal activity of the antiprotozoal drug miltefosine against *Streptococcus pneumoniae* and other pathogenic streptococci. Antimicrob Agents Chemother. 2007;51(5):1844-1848.
12. Widmer F, Wright LC, Obando D, Handke R, Ganendren R, Ellis DH, Sorrell TC. Hexadecylphosphocholine (miltefosine) has broad-spectrum fungicidal activity and is efficacious in a mouse model of cryptococcosis. Antimicrob Agents Chemother. 2006;50(2):414-421.
13. Chugh P, Bradel-Tretheway B, Monteiro-Filho CM, Planelles V, Maggirwar SB, Dewhurst S, Kim B. Akt inhibitors as an HIV-1 infected macrophage-specific anti-viral therapy. Retrovirology. 2008;5:11.
14. Eissa MM, El-Azzouni MZ, Amer EI, Baddour NM. Miltefosine, a promising novel agent for *schistosomiasis mansoni*. Int J Parasitol. 2011;41(2):235-242.
15. Blaha C, Duchêne M, Aspöck H, Walochnik J. *In vitro* activity of hexadecylphosphocholine (miltefosine) against metronidazole-resistant and -susceptible strains of *Trichomonas vaginalis*. J Antimicrob Chemother. 2006;57(2):273-278.
16. Eissa MM, Amer EI. *Giardia lamblia*: A new target for miltefosine. Int J Parasitol. 2012;42(5):443-452.
17. Seifert K, Duchêne M, Wernsdorfer WH, Kollaritsch H, Scheiner O, Wiedermann G, et al. Effects of miltefosine and other alkylphosphocholines on human intestinal parasite *Entamoeba histolytica*. Antimicrob Agents Chemother. 2001;45(5):1505-1510.
18. Walochnik J, Duchêne M, Seifert K, Obwaller A, Hottkowitz T, Wiedermann G, et al. Cytotoxic activities of alkylphosphocholines against clinical isolates of *Acanthamoeba* spp. Antimicrob Agents Chemother. 2002;46(3):695-701.
19. Polat ZA, Obwaller A, Vural A, Walochnik J. Efficacy of miltefosine for topical treatment of *Acanthamoeba* keratitis in Syrian hamsters. Parasitol Res. 2012;110(2):515-520.
20. Schuster FL, Guglielmo BJ, Visvesvara GS. *In-vitro* activity of miltefosine and voriconazole on clinical isolates of free-living amebas: *Balamuthia mandrillaris*, Acanthamoeba spp., and Naegleria fowleri. J Eukaryot Microbiol. 2006;53(2):121-126.
21. Garg R, Tremblay MJ. Miltefosine represses HIV-1 replication in human dendritic cell/T-cell cocultures partially by inducing secretion of type-I interferon. Virology. 2012;432(2):271-276.
22. Ni Nyoman AD, Lüder CG. Apoptosis-like cell death pathways in the unicellular parasite *Toxoplasma gondii* following treatment with apoptosis inducers and chemotherapeutic agents: a proof-of-concept study. Apoptosis. 2013;18(6):664-680.
23. World Health Organization (2019). World Health Organization model list of essential medicines: 21st list 2019. Geneva: World Health Organization. hdl:10665/325771. WHO/MVP/EMP/IAU/2019.06. License: CC BY-NC-SA 3.0 IGO.
24. Eissa MM, Barakat AM, Amer EI, Younis LK. Could miltefosine be used as a therapy for toxoplasmosis? Exp Parasitol. 2015;157:12-22.
25. Mohammad Mehdi M, Seyed Mohsen F, Reza A. Brinzolamide-Loaded Nanoemulsions: *In vitro* release evaluation. Iran J Pharm Sci. 2016;12(3):75-93.
26. Shafiq S, Shakeel F. Stability and self-nanoemulsification efficiency of ramipril nanoemulsion containing labrasol and plurol oleique. Clinical Research and Regulatory Affairs. 2010 Mar 1;27(1):7-12.
27. Butani D, Yewale C, Misra A. Amphotericin B topical microemulsion: Formulation, characterization and evaluation. Colloids Surf B Biointerfaces. 2014;116:351-358.
28. Ebrahimzadeh MA, Taheri MM, Ahmadpour E, Montazeri M, Sarvi S, Akbari M, Daryani A. Anti-*Toxoplasma* effects of methanol extracts of feijoa sellowiana, quercus castaneifolia, and allium paradoxum. J Pharmacopuncture. 2017;20(3):220-226.
29. Khamesipour F, Razavi SM, Hejazi SH, Ghanadian SM. *In vitro* and *in vivo* Anti-*Toxoplasma* activity of Dracocephalum kotschyi essential oil. Food Sci Nutr. 2021;9(1):522-531.
30. Montazeri M, Emami S, Asgarian-Omran H, Azizi S, Sharif M, Sarvi S, et al. *In vitro* and *in vivo* evaluation of kojic acid against *Toxoplasma gondii* in experimental models of acute toxoplasmosis. Exp Parasitol. 2019;200:7-12.
31. Coelho AC, Trinconi CT, Costa CH, Uliana SR. *In vitro* and *in vivo* miltefosine susceptibility of a *Leishmania amazonensis* isolate from a patient with diffuse cutaneous leishmaniasis. PLoS Negl Trop Dis. 2014;8(7):e2999.
32. Barbosa BF, Gomes AO, Ferro EA, Napolitano DR, Mineo JR, Silva NM. Enrofloxacin is able to control *Toxoplasma gondii* infection in both *in vitro* and *in vivo* experimental models. Vet Parasitol. 2012;187(1-2):44-52.
33. Shah J, Nair AB, Jacob S, Patel RK, Shah H, Shehata TM, Morsy MA. Nanoemulsion based vehicle for effective ocular delivery of moxifloxacin using experimental design and pharmacokinetic study in rabbits. Pharmaceutics. 2019;11(5).
34. Fouad SA, Basalious EB, El-Nabarawi MA, Tayel SA. Microemulsion and poloxamer microemulsion-based gel for sustained transdermal delivery of diclofenac epolamine using in-skin drug depot: *in vitro*/*in vivo* evaluation. Int J Pharm. 2013;453(2):569-578.
35. Garcia CR, Malik MH, Biswas S, Tam VH, Rumbaugh KP, Li W, Liu X. Nanoemulsion delivery systems for enhanced efficacy of antimicrobials and essential oils. Biomater Sci. 2022;10(3):633-653.
36. Chavhan SS, Petkar KC, Sawant KK. Simvastatin nanoemulsion for improved oral delivery: Design, characterisation, *in vitro* and *in vivo* studies. J Microencapsul. 2013;30(8):771-779.

37. Altaani BM, Almaaytah AM, Dadou S, Alkhamis K, Daradka MH, Hananeh W. Oral delivery of teriparatide using a nanoemulsion system: Design, *in vitro* and *in vivo* evaluation. Pharm Res. 2020;37(4):80.
38. Laxmi M, Bhardwaj A, Mehta S, Mehta A. Development and characterization of nanoemulsion as carrier for the enhancement of bioavailability of artemether. Artif Cells Nanomed Biotechnol. 2015;43(5):334-344.
39. Nemati S, Mohammad Rahimi H, Hesari Z, Sharifdini M, Jalilzadeh Aghdam N, Mirjalali H, Zali MR. Formulation of Neem oil-loaded solid lipid nanoparticles and evaluation of its anti-*Toxoplasma* activity. BMC Complement Med Ther. 2022;22(1):122.
40. Sanfelice R, Bortoleti B, Tomiotto-Pellissier F, Silva TF, Bosqui LR, Nakazato G, et al. Biogenic silver nanoparticles (AgNp-Bio) reduce *Toxoplasma gondii* infection and proliferation in HeLa cells, and induce autophagy and death of tachyzoites by apoptosis-like mechanism. Acta Trop. 2021;222:106070.
41. Azami SJ, Amani A, Keshavarz H, Najafi-Taher R, Mohebali M, Faramarzi MA, et al. Nanoemulsion of atovaquone as a promising approach for treatment of acute and chronic toxoplasmosis. Eur J Pharm Sci. 2018;117:138-146.
42. Adeyemi OS, Murata Y, Sugi T, Kato K. Inorganic nanoparticles kill *Toxoplasma gondii* via changes in redox status and mitochondrial membrane potential. Int J Nanomedicine. 2017;12:1647-1661.
43. Arruda da Silva Sanfelice R, Silva TF, Tomiotto-Pellissier F, Bortoleti B, Lazarin-Bidóia D, Scandorieiro S, et al. Biogenic silver nanoparticles reduce *Toxoplasma gondii* infection and proliferation in RAW 264.7 macrophages by inducing tumor necrosis factor-alpha and reactive oxygen species production in the cells. Microbes Infect. 2022;24(5):104971.
44. Quan JH, Gao FF, Ismail H, Yuk JM, Cha GH, Chu JQ, Lee YH. Silver nanoparticle-induced apoptosis in ARPE-19 cells is inhibited by *Toxoplasma gondii* pre-infection through suppression of NOX4-dependent ROS generation. Int J Nanomedicine. 2020;15:3695-3716.